Catalysis Science & Technology

Accepted Manuscript

This article can be cited before page numbers have been issued, to do this please use: M. Kumar and S. Sharma, *Catal. Sci. Technol.*, 2025, DOI: 10.1039/D5CY00021A.

ROYAL SOCIETY OF CHEMISTRY

rsc.li/catalysis

View Article Online
DOI: 10.1039/D5CY00021A

Natural Kaolin Derived Ruthenium Supported Nanoporous Geopolymer: A Sustainable Catalyst for CO_2 Methanation

Mukesh Kumar and Sudhanshu Sharma*

Department of Chemistry, Indian Institute of Technology Gandhinagar, Palaj, 382355, India

*Corresponding author - Email: ssharma@iitgn.ac.in, https://orcid.org/0000-0002-5217-9941

ABSTRACT

Addressing the serious concern of excessive CO_2 emission, CO_2 methanation reaction for converting environmental CO_2 to methane is a suitable way. Methane can be used not only as a fuel but also as a hydrogen carrier. In this study, the geopolymer is explored as a support which is synthesized using natural kaolin (GNK). This geopolymer support is used to disperse ruthenium (Ru) nanoparticles by a single-step hydrazine reduction method. The catalyst is characterized using various surface and bulk techniques. Further, the catalytic performance of ruthenium-supported Geopolymer (Ru/GNK) for CO_2 methanation process is explored with varying Ru % loading and with varying flow rates. Catalyst stability is also checked for 20 h by time on stream isothermal experiment. The spent catalyst is characterized by O_2-temperature programmed oxidation (O_2-TPO) and X-ray photoelectron spectroscopy. Overall, the catalyst proved to be cost-effective and free from pretreatment requirement apart from the superior activity, high selectivity, and good stability.

1. INTRODUCTION

The development of renewable energy generation has accelerated over the world. Global warming caused by excessive fossil fuel consumption and their decreasing availability heightens the urgency of securing clean and renewable energy resources. [1] Despite advances in photovoltaic[2] and wind generation technology[3], their daily and seasonal intermittent availability continues to be a major barrier, both in terms of consistent energy supply and

View Article Online
DOI: 10.1039/D5CY00021A

accompanying infrastructures. Several reports revealed that CO_2 is one of the major components of burning fossil fuel, and its increasing concentration is responsible for global warming. Thus, CO_2 mitigation has become a major concern. One of the possible ways by which we can mitigate environmental CO_2 is the methanation of CO_2 to form methane (CH_4). As the process of methanation requires hydrogen and its storage has many problems, so hydrogen which can be generated by electrolysis using renewable energy can be utilized for the CO_2 methanation. CH_4 thus formed contains a high weight percent of hydrogen (25%) and solves the problem of hydrogen storage as well.

CO_2 methanation reaction is highly exothermic and thermodynamically favored at low temperatures. However, catalysts are necessary to lower the high activation barriers and to alter the kinetics of the reaction. As per literature, several catalysts are available for this process. where active metals such as Ru, Rh, Pt, Ni, and Pd -supported over oxides like SiO_2, Al_2O_3, ZrO_2, TiO_2, and CeO_2.[4] Noble metals like Ru, Rh, Pt and Pd are reported to be highly active for CO_2 methanation.[1] Also, these metals are resistant towards deterioration due to sulphur poisoning, carbon deposition, and carbide formation.[5]

Working with 5 wt % noble metal alumina-supported catalysts, as reported by Solymosi and Erdöhelyi, the rate of CO_2 methanation follows the order: Ru > Rh > >Pt~Ir~Pd. Apart from it, majority of the studies reported that Ru based catalysts are highly efficient towards CO_2 conversion showing high CH_4 yield and selectivity. Further, they are also stable over longer duration of time. Due to minimal metal loading requisite for supported metal catalysts as compared to bulk catalysts they appear to be an economically viable choice.[6] The characteristics of the catalytic support such as morphology, pore structures and surface area, significantly affect the metal dispersion over it and thus alter the reaction performance.[7]

In the CO_2 methanation reaction, the chemical properties such as acidity and basicity of the support do affect the carbon dioxide adsorption capacity.[8] Catalytic supports derived from pure

View Article Online
DOI: 10.1039/D5CY00021A

chemicals, including SiO_2, Al_2O_3, CeO_2, and zeolites, have been extensively reported for CO_2 methanation.[9] Natural materials such as kaolin clay and dolomite are cost efficient and environmentally benign so they qualify to be used as the support. Kaolin, the natural clay has been studied for CO_2 methanation. Aimdate et al. studied kaolin as support for CO_2 methanation and they did CeO_2 promotion and microwave-assisted hydrothermal synthesis to increase the CO_2 conversion.[10] The challenges associated with the usage of kaolin includes its low surface area and acidic surface. Nevertheless kaolin can be used as a raw material for the preparation of geopolymer which is more basic in nature and has higher surface area and porosity.[11]

Geopolymers are inorganic polymers that are prepared by treating various aluminosilicates with hydroxides, silicates, or carbonates of alkali and alkaline earth metals.[12] These materials have a three-dimensional network of AlO_4 and SiO_4 tetrahedra connected by oxygen corners and are amorphous or semicrystalline.[13] Geopolymer has a tunable surface area and can be a potential support for fine metal dispersion. Geopolymer's stability at high temperatures (1000-1200 °C) makes it suitable for the demanding conditions. The ability to adjust acidity and basicity by controlling hydroxyl ion ratios influences CO_2 adsorption during processes like methanation. Thus, geopolymer presents a cost-efficient, adaptable, and thermally stable support for various applications. However, there are very few reports on the use of geopolymers as catalyst supports. Therefore, it is necessary to further study the role of geopolymers as a support in catalysis, which will be helpful for the development and application of geopolymer-based catalysts. Here, we report natural kaolin-derived geopolymer as a support for CO_2 methanation. In this study, geopolymer, prepared from alkali (KOH) activation of metakaolin derived from natural kaolin is used as a support for Ru nanoparticles. This is a novel and economical approach that has not been explored earlier to the best of our knowledge. Further, yield and carbon balance is usually not reported in literature and our analysis includes detailed

View Article Online
DOI: 10.1039/D5CY00021A

mole-to-mole conversion calculations of reactants to products, providing critical insights into the reaction's efficiency and carbon utilization.

2. MATERIALS & METHODS

2.1 Catalyst Synthesis

Kaolin powder was calcined at 750 °C for 10 h to obtain metakaolin with increasing reaction activity for polymerization. To prepare geopolymer from metakaolin, firstly the aqueous solution of KOH was prepared by dissolving 14 g of KOH in 32 mL of distilled water. Then 15.43 g of fumed silica was added to the aqueous solution of KOH and stirred with a mechanical stirrer for 30 min at 800 rpm to make a clear solution. Further, 10 g of metakaolin was added slowly and dissolved properly. The resulting resin was cured in an oven at 60 °C for 24 h.[11] A brown-coloured (geopolymer) cured product was broken into sample pieces and crushed into fine powder and then washed with DI water several times to remove the excess of alkali. This scheme is shown in **Figure 1(a).**

As shown in **Figure 1(b)** for dispersion of Ru on Geopolymer, 0.75 g of geopolymer was taken in a round bottom flask. 20 mL of DI water was added to it and sonicated for 30 min. As per requirement (for different Ru % loading), add the required volume of 1wt % solution of $RuCl_3.3H_2O$ and sonicate it again for 30 min. Next, add 20 mL of hydrazine hydrate (99-100%) drop by drop under continuous stirring. After the complete addition of hydrazine hydrate, leave this solution on stirring for 6 h so that there is a complete reduction of Ru (3+) to Ru (0). The obtained solution was filtered and washed with DI water for 4-5 times. The solid that remains after filtration was dried at 60 °C for 24 h. A brown color powder formed, which is Ru supported over Geopolymer (Ru/GNK), which will be used for catalysis without further pretreatment.

View Article Online
DOI: 10.1039/D5CY00021A

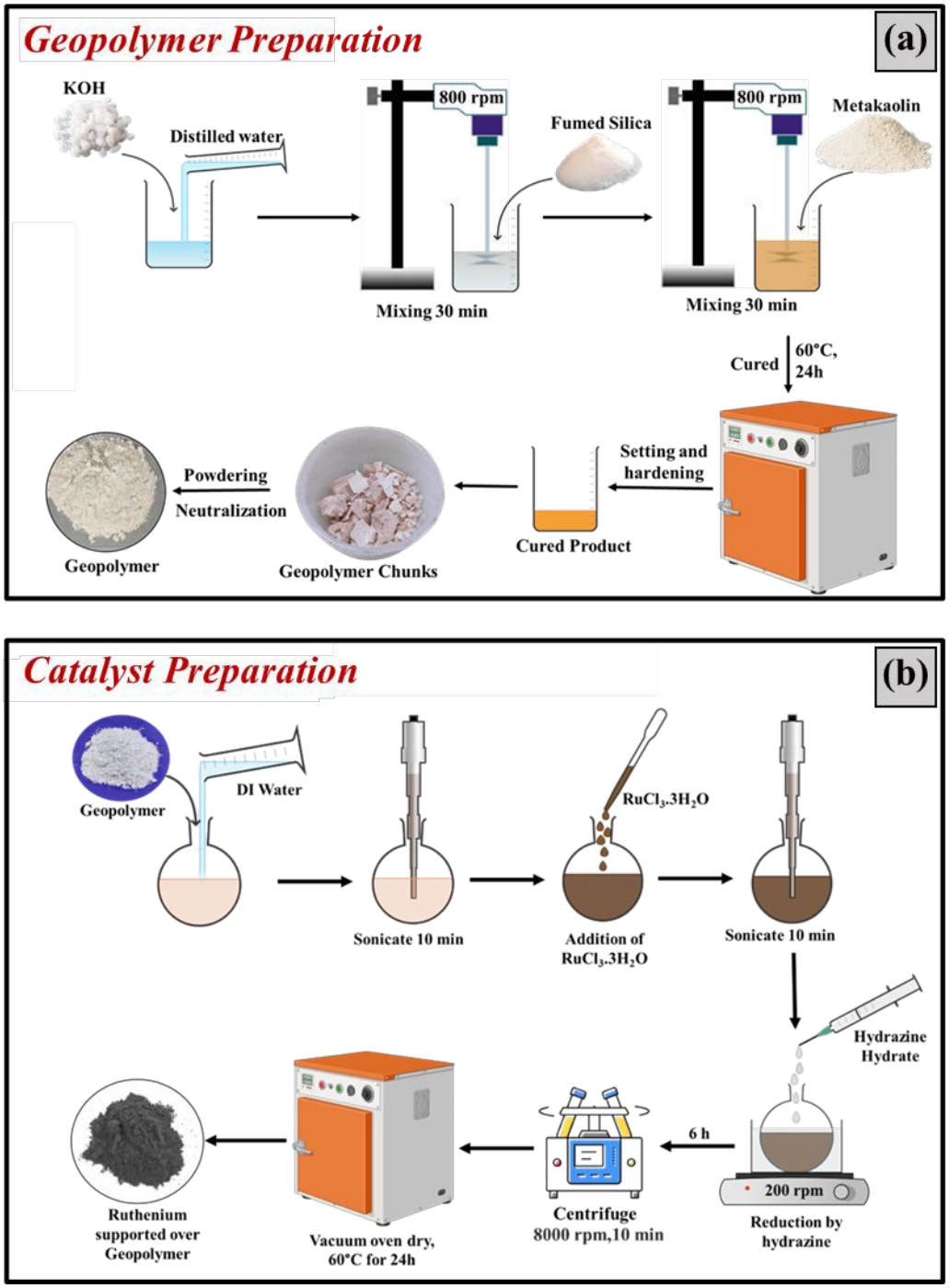

Figure 1. (a) Schematic representation of geopolymer preparation from natural kaolin. (b) Scheme showing the deposition of Ru nanoparticle on geopolymer.

View Article Online
DOI: 10.1039/D5CY00021A

2.2 Characterization of catalyst

The synthesized Ru supported on geopolymer catalysts was characterized by X-ray diffraction (XRD), using a Bruker D8 Discover diffractometer. The diffractometer was equipped with Cu Kα radiation (λ = 1.5406 Å), the analysis was carried out in the 2θ range of 10 to 70 degrees with a scan speed of 2 degree/min. High resolution Transmission Electron Microscopic (HR-TEM) pictures were obtained utilizing a Thermo Titan Themis 300 kV at an accelerating voltage of 200 kV in order to understand the formation of Ru nanoparticles over geopolymer. For the preparation of TEM sample the catalyst was first dispersed in methanol using ultrasonication. Then the dispersed catalyst was drop casted over the carbon coated copper grid and dried for 1 h. For the calculation of particle size and d-spacing, imageJ software was used. JEOL JSM-7900F, Field Emission Scanning Electron Microscope (FE-SEM), was used for analysis of sample morphology. An energy-dispersive X-ray spectrometer (EDS) instrument attached to the FE-SEM, with AZtec (Oxford Instruments) software, was used to determine elemental composition.

The specific surface area of prepared catalyst was studied using Micromeritics 3 Flex Surface analyzer. Before the measurement the sample were preheated to remove the moisture and adsorbed gases from sample. The samples were degassed in vacuum first at 90°C for 1 h and then at 350 °C for 4 h. The Brunauer–Emmett–Teller (BET) method was applied to calculate the specific surface area of the samples. Fourier transform infrared spectroscopy (FTIR) was used to analyze functional groups present in the materials using Perkin Elmer (UATR two). The Ruthenium (Ru) concentrations in the catalyst were measured using ICP-OES (Perkin Elmer, Avios 200). For this, Ru geopolymer was first digested with aqua regia to make it a clear solution; after this, water was added to make it a 100 ppm solution. To find the oxidation state of Ru in the catalyst X- ray photoelectron spectroscopy was done by using AXIS Ultra

View Article Online
DOI: 10.1039/D5CY00021A

DLD spectrometer (Kratos) with a monochromatic Al Kα radiation (hv =1486.6 eV) as the excitation source.

The reducibility of the catalyst has been checked by performing H_2-TPR experiment using TCD detector (CIC-Binary Gas Analyzer, Baroda, India). The basicity of the catalyst was checked by CO_2-temperature programmed desorption using FID detector (CIC-Binary Gas Analyzer, Baroda, India). CO_2 gas was first adsorbed on the catalyst with a flow rate of 30 mL/min for 30 min at room temperature. The catalyst was then flushed with nitrogen for 10 min to remove the weakly adsorbed CO_2. At last, the catalyst was heated from 30 to 700 °C at a constant heating rate of 10 °C/min in the presence of nitrogen.

2.3 Catalytic Activity Test

The catalytic activity of Ru/GNK was tested in a packed bed micro flow reactor with 50 mg catalyst. The quartz tube (25 cm length, 4 mm internal diameter), loaded with the catalyst packed with quartz wool, was placed in a tubular furnace with temperature control. CO_2 methanation reactions were conducted with 10% CO_2 + 90% N_2 and 10% H_2 + 90% N_2, maintaining a 1 : 4 = CO_2 : H_2 ratio. Additional nitrogen was added to maintain the overall flow rate. Reaction conditions ranged from room temperature to 500 °C with space velocities from 20,000 to 60,000 h^{-1}. A K-type thermocouple measured the catalytic bed temperature. Gas analysis was done by using CIC Dhruva gas chromatography instrument. The standard calibration cylinder was used to calculate the number of moles of the reactants and products. These moles were used to calculate the conversions, yield, selectivity, and carbon balance using SI equations (1), (2), and (3).

2.4. Analysis of spent catalyst

Spent 3%Ru/GNK after 20 h of long-term stability test was characterized by O_2-temperature programmed oxidation (O_2-TPO) and XPS. O_2-TPO was carried out to estimate the deposited carbon on the catalyst. O_2-TPO is performed on the same setup that was used in CO_2-TPD. The

View Article Online
DOI: 10.1039/D5CY00021A

catalyst was flushed with nitrogen for 10 min to remove the weakly adsorbed gases. Then it was heated from 30 to 700 °C at a constant heating rate of 10 °C/min in the presence of oxygen.

3. RESULTS AND DISCUSSION

3.1. Material Characterization

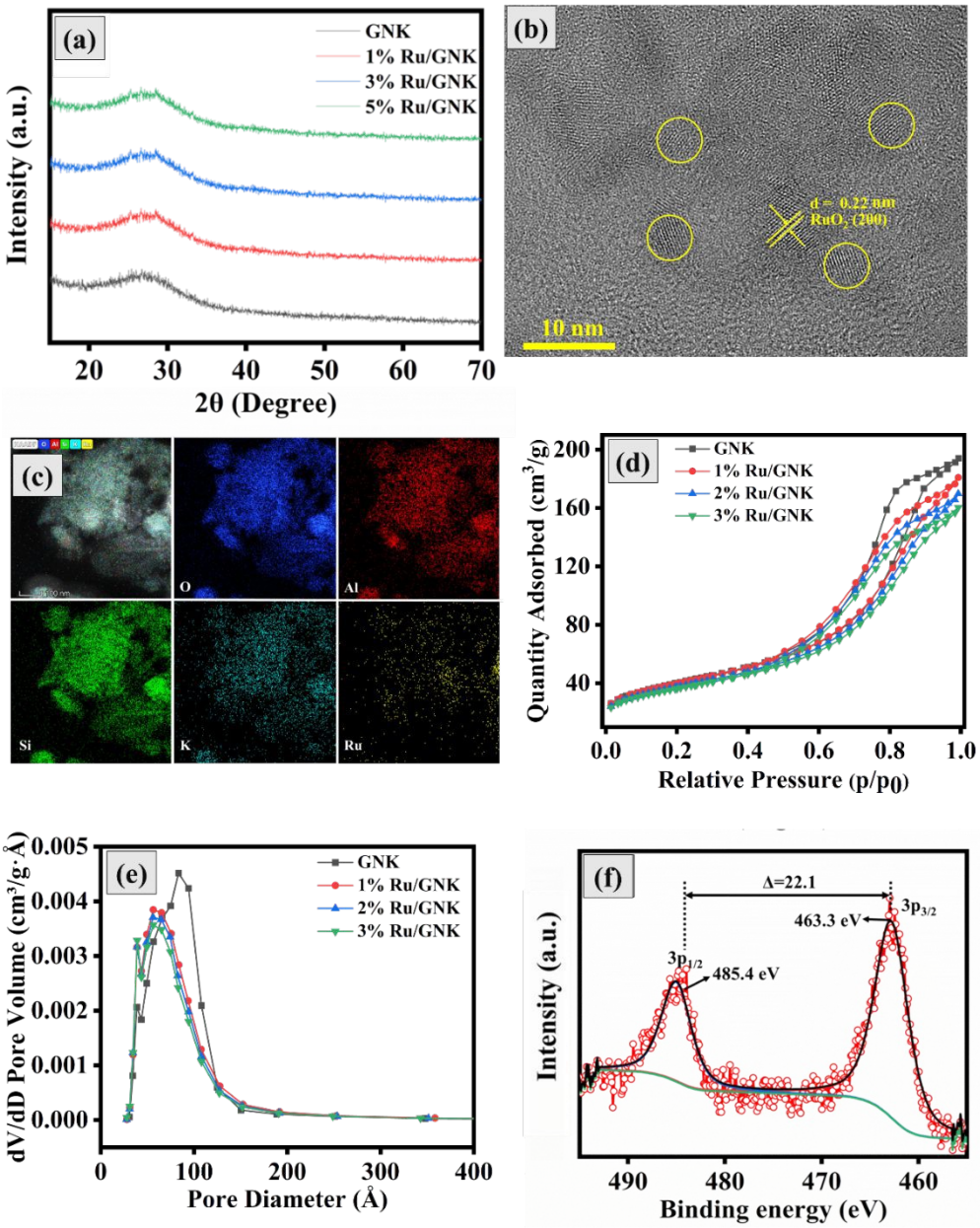

Figure 2. (a) X-ray diffraction pattern (XRD) of geopolymer from natural kaolin (GNK) and Ru supported over geopolymer from natural kaolin (Ru/GNK) with Ru loading of 1%, 3% and 5% (b) HR-TEM image of Ru nanoparticle on geopolymer support (GNK) in 3% Ru/GNK (c) HAADF-STEM image, corresponding EDS element mapping showing the distribution of Ru` over the geopolymer support in 3% Ru/GNK (d) N_2-sorption isotherms and, (e) and BJH desorption dV/dD pore volume vs pore diameter curves of GNK and 1%, 3% and 5% Ru/GNK (f) X-ray photoelectron spectroscopy (XPS) profile of Ru 3p of 3% Ru/GNK

View Article Online
DOI: 10.1039/D5CY00021A

X-ray diffraction patterns of synthesized catalyst are obtained in the range of 2θ from 10°-70° as shown in **Figure 2(a)**. From the XRD analysis, as shown in **Figure S1**, it was observed that natural kaolin (NK) consisted of kaolinite, quartz, and a small amount of illite phase.[14] On heating kaolin at 750°C, the crystalline structure changes to an amorphous metakaolin (MK) structure. MK prepared from the calcination of NK is used to prepare the geopolymer. Geopolymer prepared from NK is amorphous and shows a small hump in the lower 2θ range. For all Ru/GNK with different amounts of Ru loading, no peak corresponds to Ru and RuO_2 is observed in the XRD pattern which may be due to very small amount Ru on the geopolymer or high dispersion of small-sized Ru on Geopolymer not detectable in XRD.

HR-TEM images of 3% Ru/GNK reveal the presence of crystalline RuO_2 on the GNK support, as shown in **Figure 2(b).** Since the support material is amorphous, we are not getting any lattice fringes corresponding to the support material. The yellow-colored circle corresponds to crystalline Ru dispersed over GNK. The calculated d-spacing value of 0.22 nm corresponds (200) plane of RuO_2 in 3% Ru/GNK. The average particle size of RuO_2 was calculated as 2.4 nm. So, the TEM analysis confirms that RuO_2 is present in the crystalline form and is uniformly distributed on the surface of GNK. Considering that the particle size is very small, it was not detected during the XRD analysis. HAADF-STEM image of 3% Ru/GNK in **Figure 2(c)**, corresponding EDS element mapping showing the distribution of Ru over the geopolymer. From this image it is confirmed that Ru is uniformly distributed over the geopolymer.

The actual weight percentage of ruthenium over geopolymer is confirmed by ICP-OES, which is given in **Table 1.** The ICP-OES results show that the estimated amount of deposited metal is close to the calculated value in case of 1% and 3% Ru/GNK, but the value is less than expected in the case of 5% Ru/GNK. It is possible that the geopolymer surface is not able to accommodate the larger amount of Ru nanoparticles, and extra nanoparticles either wash off or remain in the solution phase without deposition.

View Article Online
DOI: 10.1039/D5CY00021A

Table 1. ICP-OES, SEM-EDX and N_2 adsorption-desorption results of the catalyst

Catalyst Name	ICP-OES Metal Loading (wt. %)	Wt. % from SEM-EDX	BET Surface Area (m^2/g)	Pore Volume (cm^3/g)	Pore Size (Å)
GNK	-	-	141.7	0.305	77.2
1% Ru/GNK	0.9	1.8	140.5	0.286	73.6
3% Ru/GNK	2.8	3.9	132.4	0.268	72.2
5% Ru/GNK	4.0	4.9	127.9	0.253	71.5

N_2 adsorption-desorption measurement is done to evaluate the surface area, pore volume, and pore size of support (GNK) and Ru metal deposited over support (Ru/GNK). As shown in the **Figure 2(d)** GNK and Ru/GNK belongs to type-IV adsorption isotherms and type-H2(b) hysteresis loops.[15] The mesoporous architectures of the GNK and Ru/GNK catalysts were clearly visible in the graph of pore size distributions measured by BJH as shown in **Figure 2(e)**. The surface area of GNK is 141.7 m^2/g. After the deposition of Ru metal on the support (Ru/GNK), a decrease in surface is observed as compared with GNK. The surface area of 1%Ru/GNK, 3%Ru/GNK and 5%Ru/GNK is 140.5 m^2/g, 132.4 m^2/g and 127.9 m^2/g respectively. Loading of Ru nanoparticles on the support partially blocks the pores, resulting in a decrease in surface area, pore volume, and pore size of Ru/GNK compared to GNK support. The specific surface area, pore volume, and pore size of the catalyst are shown in **Table 1**.

The NK has a sheet-like structure, and when heated at 750 °C, it gets converted into MK, where the sheet-like structure gets destroyed, as shown in **Figure SI3**. When MK is utilized for the

View Article Online
DOI: 10.1039/D5CY00021A

preparation of geopolymer, no significant changes are observed. Even after the deposition of Ru on the GNK, negligible change is observed in the shape size and overall morphology of the geopolymer, as shown in **Figures SI4, SI5, and SI6**. This indicates that the size of Ru nanoparticle deposited over GNK is very small in size, so no change in the size of the GNK is observed. As shown in **Figures SI4, SI5, and SI6** there is no particular shape of particles in all three Ru/GNK catalysts with different Ru loading. All three catalysts have almost similar morphology

XPS analysis was carried out to investigate the components chemical states over the prepared catalyst surface. The XPS survey scan spectrum of Ru/GNK reveals the presence of all expected elements, such as Ru, Al, Si, C, and O, as shown in **Figure SI7**. In the overall XPS survey, the overlapping of peaks at around 285 eV for C 1s and Ru 3d leads to difficulties in the analysis of ruthenium; thus, Ru(3p) was chosen for the analysis. **Figure 2(f)** shows the Ru(3p) XPS spectra for the 3%Ru/GNK catalyst. The doublet can be deconvoluted into a pair of peaks, in which the energy values are 463.3 eV for $3p_{3/2}$ and 485.4 eV for $3p_{1/2}$. This observed

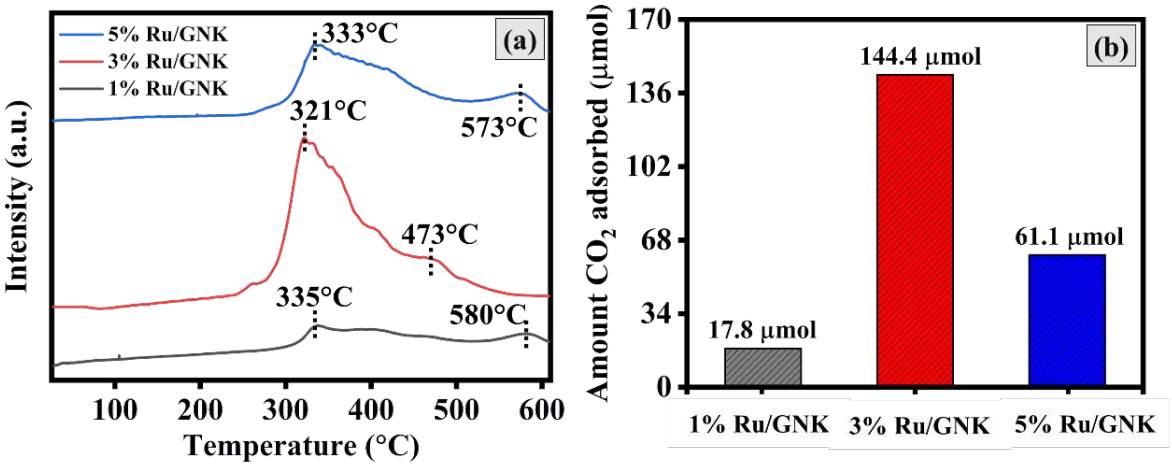

Figure 3. (a) CO_2-Temperature Programmed Desorption (CO_2-TPD) profile and (b) Adsorption capacity for CO_2 of 1%Ru/GNK, 3%Ru/GNK and 5%Ru/GNK. Reaction conditions : Amount of catalyst = 50 mg, P = 1atm, T = RT to 600°C.

View Article Online
DOI: 10.1039/D5CY00021A

data is indicative of RuO_2, which is in agreement with the data reported in the literature.[16, 17] This means that Ru nanoparticles undergo surface oxidation in the air to form RuO_2.[18]

To check the reducibility of the catalyst H_2-TPR studies have been done and given in **Figure SI 8**. Which also suggests that Ru is present as RuO_2 on the surface of the catalyst.

CO_2 temperature-programmed desorption (CO_2-TPD) experiments were conducted to determine the basicity of the Ru-Geopolymer. The results, depicted in the **Figure 3(a)** reveal two distinct peaks representing the adsorption of CO_2 on alkaline sites of different types in all three catalysts. The peak observed in the temperature range of 250-450 °C corresponds to a moderate alkaline site, while the peak observed in the range of 550-600 °C corresponds to strong alkaline site. These peaks indicate the formation of distinct carbonate species resulting from the adsorption of CO_2 on the alkaline sites. It is obvious from the **Figure 3(a) and (b)** that 3% Ru/GNK is most basic in the all catalyst because the amount CO_2 adsorbed is maximum in this case. It is also possible that at this composition, dispersion is uniform and adequate which provides large number of active sites for CO_2 to adsorb. Also, the peak which corresponds to strong alkaline site is not present in 3%Ru/GNK as shown in the **Figure 3(a)**. For catalysis strongly alkaline sites are not useful as it will violate the moderation principle.[19]

View Article Online
DOI: 10.1039/D5CY00021A

3.2. Catalytic Activity Test

3.2.1 Catalytic performance with different % Ru loading

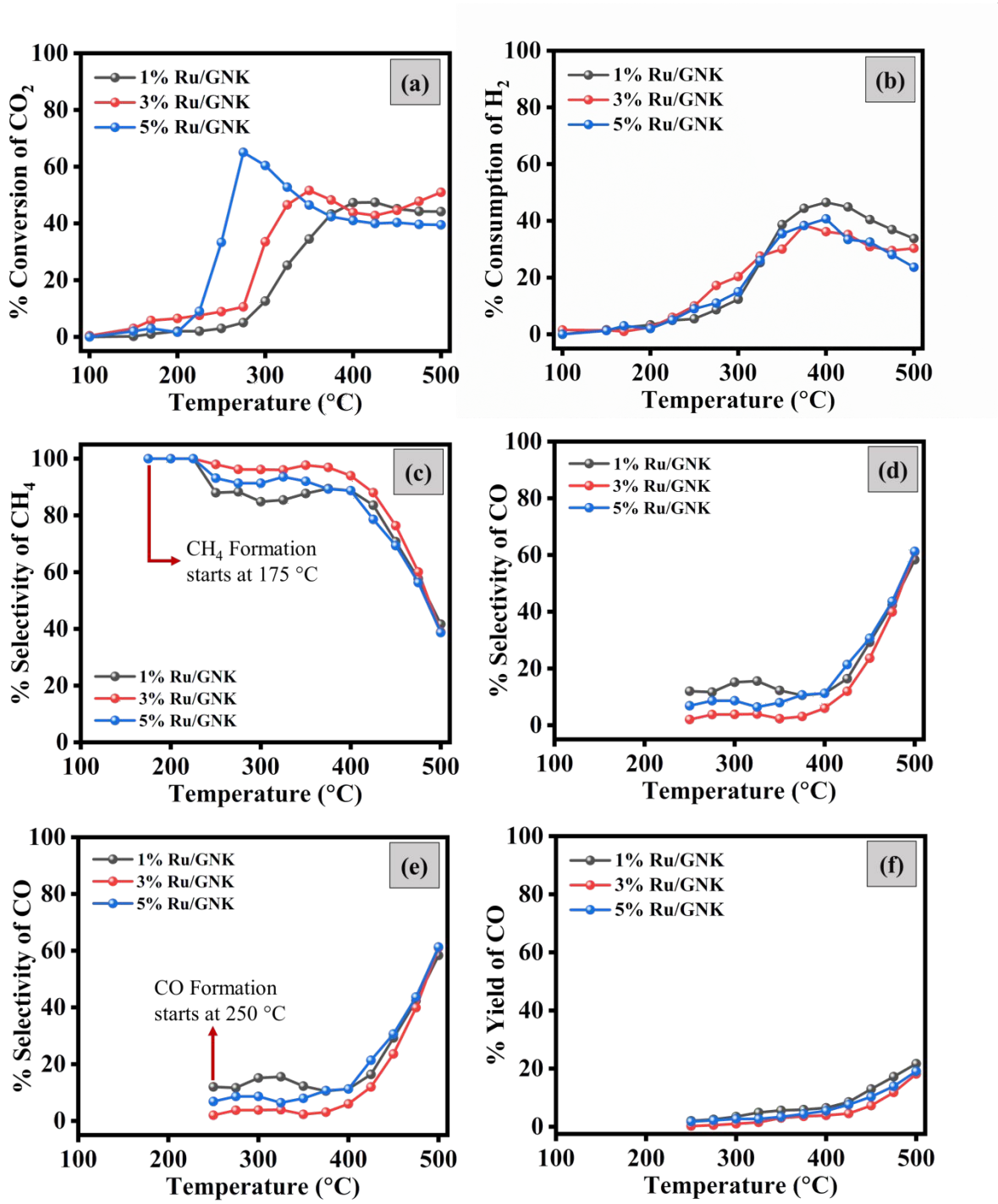

Figure 4. Catalytic activity test with different wt.% of Ru on geopolymer from natural kaolin (GNK) (a) CO_2 conversion (b) H_2 consumption (c) CH_4 selectivity (d) CH_4 yield (e) CO selectivity (f) CO yield. Reaction conditions: Amount of catalyst = 50mg, P = 1 atm, T = RT to 500°C, GHSV = 20,000 h^{-1} and (H_2/CO_2) ratio = 4.

View Article Online
DOI: 10.1039/D5CY00021A

The activity of the catalyst is evaluated by performing CO_2 methanation from the temperature 100 °C to 500 °C with different amounts of Ru loading on GNK. **Figure 4** shows the catalytic activity of Ru/GNK with different loading percentages of Ru. In all three cases, the CO_2 conversion started at around 175 °C, CH_4 formation also started at 175 °C, and CO formation, the side product of CO_2 methanation, is forming at 250 °C. In case of 1%Ru/GNK the maximum CO_2 conversion is 47.4% at 425 °C, CH_4 selectivity is 83.6%, CH_4 yield is 35.8%. In case of 3%Ru/GNK maximum CO_2 conversion is increasing to 51.6% at 350 °C, CH_4 selectivity is 97.7%, CH_4 yield is 41.8%. In case of 5%Ru/GNK we are getting maximum CO_2 conversion 65% at 275 °C, CH_4 selectivity 91.3% and CH_4 yield 7.4%. Despite of large CO_2 conversion at 275 °C, the CH_4 yield is very low (7.4%). So, there might be a possibility that CO_2 is showing adsorption behaviour without methanation. In all cases when the reaction temperature exceeds 400 °C, the CO_2 conversion and methane selectivity decrease under the influence of thermodynamics, and at the same time, the rate of the side reaction, reverse water gas shift (RWGS) reaction, $CO_2 + H_2 \rightarrow CO + H_2O$ increases.[20] Since the Sabatier reaction is an exothermic reversible reaction, with the increase in temperature, the reaction shifts in a backward direction, which is one of the reasons for the decrease in CO_2 conversion. Also, RWGS reaction dominates at higher temperatures and is responsible for lower selectivity for methane at higher temperatures. When we compare these three catalysts, we must look at the temperature requirement for CO_2 conversion, selectivity, and yield of the major product (CH_4). For the catalyst to be good, we should get maximum conversion of CO_2, maximum CH_4 selectivity, and maximum CH_4 yield at lower temperatures. If we compare these three catalysts, we get maximum conversion of CO_2 with maximum CH_4 yield and maximum selectivity of CH_4 at 350 °C for 3%Ru/GNK. So, if we compare the catalyst at 350 °C, the CO_2 conversion,

View Article Online
DOI: 10.1039/D5CY00021A

CH_4 selectivity, and CH_4 yield follow the order 3%Ru/GNK > 5%Ru/GNK > 1%Ru/GNK. Overall, 3% Ru/GNK is a preferred choice.

3.2.2 Catalytic performance with different flow rates of reactant gases

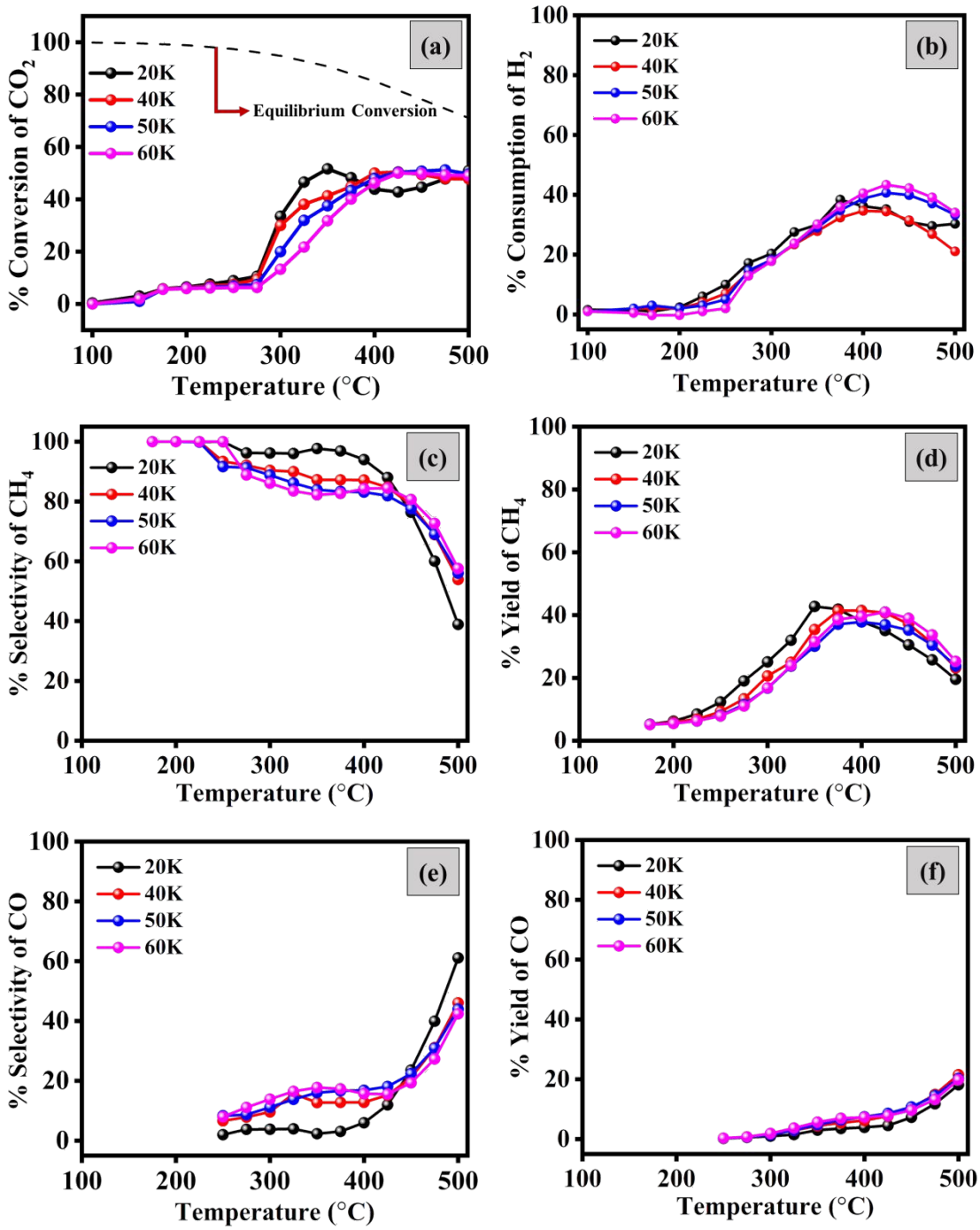

Figure 5. Effect of flow rate on the catalytic activity of 3% Ru/GNK with temperature (a) CO_2 conversion, (b) H_2 consumption (c) CH_4 selectivity (d) CH_4 yield (e) CO selectivity (f) CO yield vs temperature. Reaction conditions: Amount of catalyst = 50mg, P = 1 atm, T = RT to 500°C, GHSV = 20,000 h^{-1}, 40,000 h^{-1}, 50,000 h^{-1}, 60, 000 h^{-1} and (H_2/CO_2) ratio = 4.

View Article Online
DOI: 10.1039/D5CY00021A

The studies with different Ru loading showed that 3%Ru/GNK showed the best results among all other catalysts. To check the effect of the flow rate of reactant gases on catalytic activity, we study CO_2 methanation reaction at different gross hourly space velocity (GHSV) 20,000 h^{-1} (20K h^{-1}), 40,000 h^{-1} (40K h^{-1}), 50,000 h^{-1} (50K h^{-1}) and 60,000 h^{-1} (60K h^{-1}). **Figure 5** shows the results of CO_2 methanation. With the increase in temperature, the conversion of CO_2 increases and reaches its maximum, and then it decreases. The CO_2 methanation starts at ~175 °C and shows maximum conversion between 350 and 400 °C. For 20K h^{-1} GHSV, the optimal reaction temperature for the catalyst was 350 °C, and the CO_2 conversion was 51.6%, with a 41.8%. CH_4 yield and 97.7% CH_4 selectivity. Increasing the space velocity decreased the CO_2 conversion at the same temperature. For other space velocities (40K, 50K, and 60K h^{-1}), the CO_2 conversion at 350 °C was less than that for 20K h^{-1}. This is not unusual because contact time decreases as the flow rate increases, and thus, the conversion decreases.[21] The selectivity and yield of CH_4 also decrease with the increase in the flow rate of reactant gases. At higher GHSV, there is less chance of CO reduction to CH_4, the intermediate step of CO_2 methanation. [22] The exact reason is responsible for the higher selectivity and yield of CO with an increase in GHSV. Thermodynamic CO_2 conversion is comparatively higher than the experimental conversion at 350 °C. However, at 500 °C, the thermodynamic and experimental conversions are approaching each other.

View Article Online
DOI: 10.1039/D5CY00021A

3.2.3 Steam of time (stability) for CO_2 methanation over 3% Ru/GNK

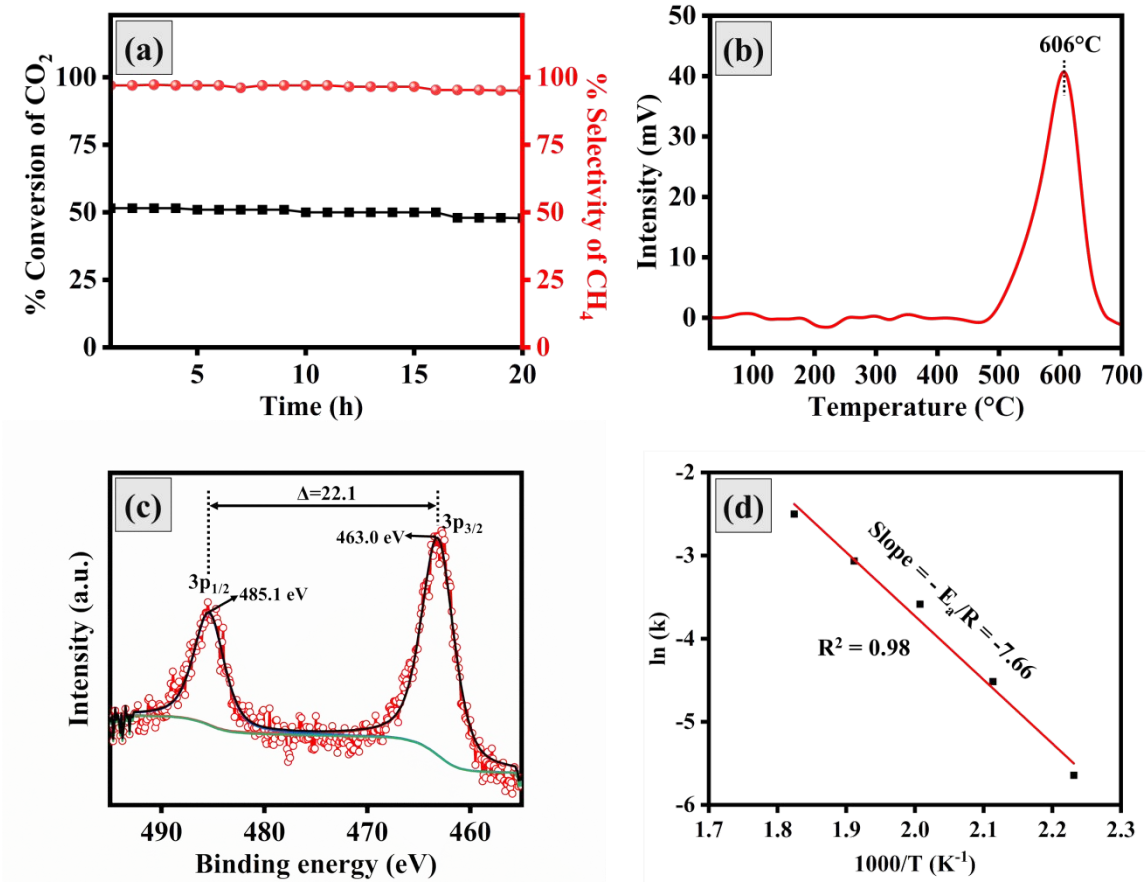

Figure 6. (a) Evolution of CO_2 conversion and selectivity of CH_4 at 350°C with time-on-stream over 20 h for 3% Ru/GNK. Reaction Conditions: Amount of catalyst taken = 50mg, P = 1 atm, T = 350°C, GHSV = 20,000 h^{-1} and (H_2/CO_2) ratio = 4 (b) O_2-Temperature programmed oxidation (O_2-TPO) (c) Ru 3p XPS profiles of spent catalyst (d) Arrhenius plot for calculation of apparent activation energy for CO_2 methanation on 3%Ru/GNK.

To examine the catalytic stability of the 3%Ru/GNK, a 20 h stability test at a constant temperature of 350 °C was conducted. As seen in **Figure 6(a)**, the 3%Ru/GNK catalyst displayed superior CO_2 conversion and long-term stability for 20 h. After 20 h, CO_2 conversion and CH_4 selectivity were decreased by ~3% and ~2%, respectively, for 3%Ru/GNK. The catalyst is stable over time, and the decrease in CO_2 conversion and CH_4 selectivity is insignificant.

View Article Online
DOI: 10.1039/D5CY00021A

4. CHARACTERIZATION OF SPENT CATALYST

4.1. O_2 – Temperature programmed oxidation (O_2-TPO)

The carbon deposition on the spent catalyst is calculated by O_2-TPO. On passing oxygen over the spent catalyst with increasing temperature from 30 to 700 °C, the formation of CO_2 is observed, as shown in **Figure 6(b)**. A weak signal confirms that carbon deposition is minimal even after 20 hours of long-term stability test. Quantitatively, only 0.078 mg/g_{cat} of Carbon is deposited under the methanation reaction conditions at the end of 20 hours. The Carbon Balance (C_B) for reactions is calculated using **SI. Equation (4)**. For all the reactions performed with 3%Ru/GNK, C_B is coming in the range of 3-6%, which means that carbon deposition in 3%Ru/GNK catalyst is minimal, and the majority of the reactant carbon forms the product.

4.2. XPS of spent catalyst

The chemical state of Ru on the surface of the spent catalyst is investigated by XPS after CO_2 methanation reactions. The Ru 3p XPS spectra for the Ru/GNK-spent catalyst is shown in **Figure 6(c)**. The Ru(3p) spectra in 3% Ru/GNK-spent can be deconvoluted into two pairs of peaks, in which the binding energy values are attributed to the $3p_{3/2}$ (463.0 eV) and $3p_{1/2}$ (485.1 eV). These values are very close to binding energies in case of fresh catalyst (3% Ru/GNK). So, there is no change in oxidation state of Ru/GNK after CO_2 methanation.

5. APPARENT ACTIVATION ENERGY CALCULATION

Using the Arrhenius relationship, the activation energy for CO_2 methanation was calculated. **Figure 6(d)** depicts the Arrhenius plot for CO_2 methanation and feed conversion in the 175–275°C temperature range for CO_2 methanation. Under kinetically controlled conditions, measurements were conducted at low conversions. The apparent activation energy for CO_2 methanation is 63.6 $KJmol^{-1}$ for 3% Ru/GNK.

View Article Online
DOI: 10.1039/D5CY00021A

On comparing with the existing literature, we found that the geopolymer support derived from natural kaolin has not been extensively reported. So, we have compared the activity of our catalyst with relatively similar catalysts in the literature in terms of CO_2 conversion, CH_4 selectivity, CH_4 yield, and apparent activation energy for CO_2 methanation, as shown in **SI Tables 1 and 2**. In our study, the reaction was carried out with 50 mg of catalyst (3%Ru/GNK), showing CO_2 conversion of 51.6%, CH_4 selectivity of 97.7%, and CH_4 yield of % at 350 °C with gas/weight hourly space velocity (GHSV/WHSV) of 20,000 h^{-1} / 39,600 $mLg^{-1}h^{-1}$. Wan et al. have reported Ni-P-SGS, a slag-based geopolymer catalyst for CO_2 methanation, which shows a CO_2 conversion of 80.2% and a CH_4 selectivity of 99.2% at 400 °C and weight hourly space velocity (WHSV) of 12,000 $mLg^{-1}h^{-1}$.[23] The conversion in their case may be high due to low WHSV i.e. higher reactant to catalyst contact time compared to our case. The geopolymer they reported is made from synthetic chemicals [$Si(OC_2H_5)4$, $Mg(NO_3)_2.6H_2O$, $Al(NO_3)_3.9H2O$, and $Ca(NO3).4H_2O$] using the sol-gel method, which is both expensive and time-consuming. In contrast, our catalyst is naturally derived from kaolin-based clay, making it more cost-effective and eco-friendly. Aimdate et al. have prepared a similar kind of catalyst using metakaolin as a support 30Ni-20Ce/MTK_M [10]. In their case, working with 100 mg of 20Ce/MTK_M catalyst, they are getting CO_2 conversion of 61.2% and a CH_4 selectivity of 98% at 350 °C and WHSV of 14,000 $mLg^{-1}h^{-1}$. Higher conversion in this case can be again due to less WHSV and more amount of catalyst taken for the reaction. Czuma et al. have reported nickel deposited over fly ash-derived zeolite, 15%Ni/Fly ash zeolite type X, as a catalyst for CO_2 methanation.[24] They are getting the CO_2 conversion of 53 % at 450 °C with GHSV of 12,000 h^{-1}. But in our case, we have achieved almost similar CO_2 conversion at a lower temperature 350 °C and higher GHSV 20,000 h^{-1}. To the best of our knowledge there is no studies where Ru based geopolymers are explored for CO_2 methanation reaction. So, it is very

View Article Online
DOI: 10.1039/D5CY00021A

difficult to compare it with reported literature. Also, the activity of the geopolymer vary with sources of kaolin clay used. In our case we have used Indian origin kaolin clay.

On comparing the apparent activation energy for CO_2 methanation, we found that it is comparable to the apparent activation energy reported for the CO_2 methanation as given in the **SI Table No. 2**. In our study, the calculated apparent activation energy for 3% Ru/GNK is 63.6 $KJmol^{-1}$. Working with similar kind of material like geopolymer Aimdate et al. have reported apparent activation energy for CO_2 methanation on 30Ni-20Ce/MTK_M catalyst as 55.1 $KJmol^{-1}$. Overall, our catalyst is comparable to the similar kind of catalyst reported in the literature.

View Article Online
DOI: 10.1039/D5CY00021A

6. TRANSIENT STUDY

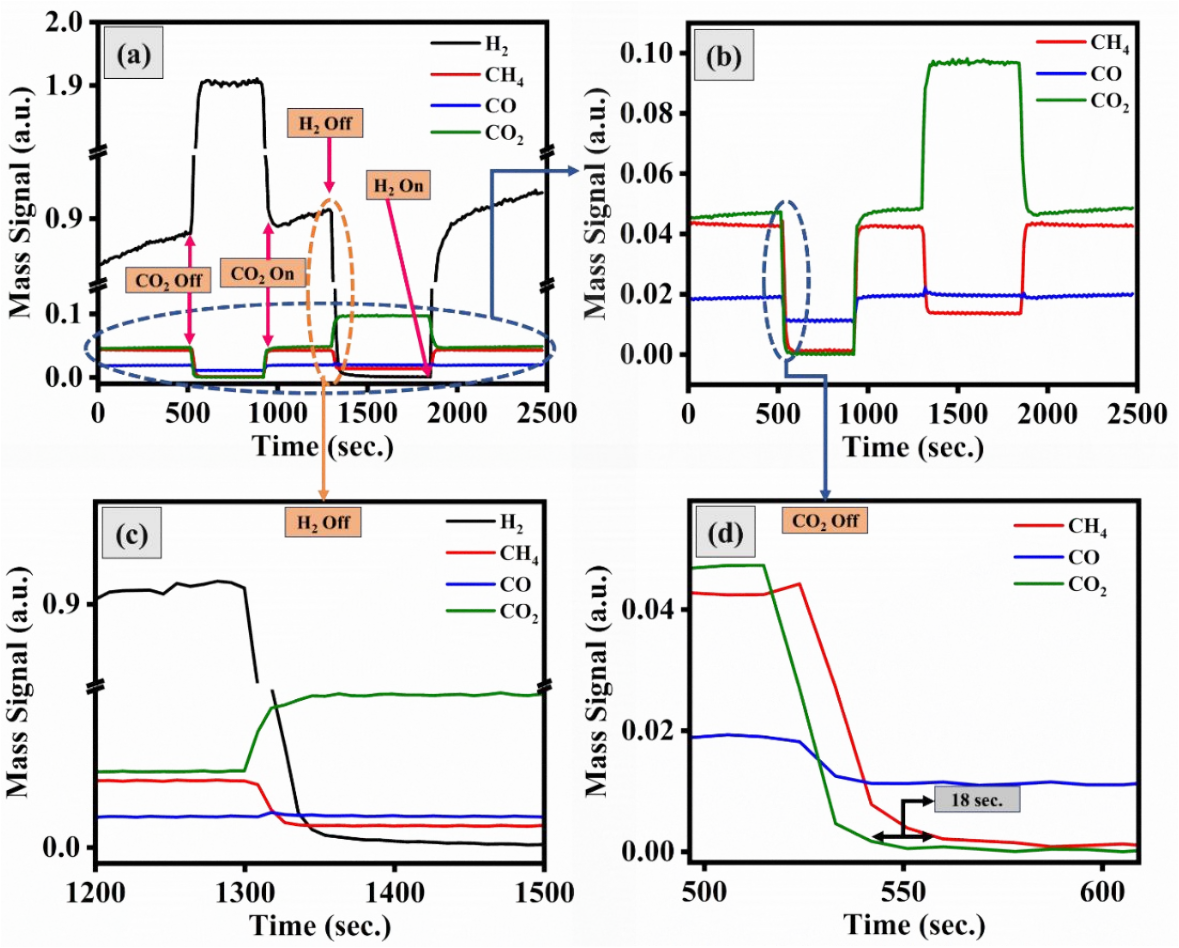

Figure 7. Transient study of CO_2 methanation on 3% Ru/GNK at 350°C at GHSV = 20,000 h^{-1}(a) Mass signal of reactant gases (CO_2 and H_2) and product gases (CH_4 and CO) and the effect of removing reactant gases on product formation (b) Magnified response of CH_4, CO and CO_2 (c) Magnified response on cutting H_2 (d) Magnified response on cutting CO_2

Transient studies were conducted to determine the dependence of methanation reaction on the reactants, i.e., CO_2 and H_2, as shown in **Figure 7**. For this, we chose the optimal conditions for the reaction i.e., 3%Ru/GNK, Temp.=350°C GHSV = 20,000 h^{-1} and (H_2/CO_2) ratio = 4. Initially, we had all reactant gases in the reaction stream, and their response was recorded using the mass spectrometer. On stopping the flow of CO_2, whilst continuing the H_2 flow; It was observed that the signal of CO_2, CH_4 and CO altogether approaches to zero. However, there was a time-lapse of 18 sec in the decrease of CH_4 response as compared to that of CO_2, which

View Article Online
DOI: 10.1039/D5CY00021A

suggests that there might be some intermediates (possibly carbonate type of species) on the surface of the catalyst that are responsible for the methanation, even though there is no CO_2 in the gas stream. Further, to investigate whether the adsorbed hydrogen participates in the reaction, we stopped the H_2 flow while continuing the CO_2 flow. We observed that CH_4 formation diminished right after the H_2 was stopped. This means that the reaction of H_2 with carbonaceous intermediate is very swift. So, there seems to be no role of chemisorbed H_2 in the methanation step.

7. CONCLUSION

In conclusion, this study investigated the utilization of a geopolymer derived from natural kaolin as a support material for CO_2 methanation. We successfully prepared a Ru-supported geopolymer catalyst (Ru/GNK) via hydrazine reduction, revealing some key findings. XRD analysis revealed the amorphous nature of the geopolymer, and the introduction of Ru onto the geopolymer did not alter its XRD pattern significantly while a small amount of Ru is noticed. TEM studies confirmed the presence of RuO_2 nanoparticles on the GNK support. ICP and SEM-EDS analyses further confirmed the presence of Ru in the catalyst. However, the deposition of Ru on the geopolymer led to a reduction in surface area, attributed to partial pore occupation by RuO_2 nanoparticles. XPS analysis provided insight into the oxidation state of Ru in the geopolymer, confirming its presence in the +4 oxidation state. Comparing various Ru loadings on the Geopolymer for CO_2 methanation, we identified 3% Ru/GNK as the catalyst that outperformed others in terms of temperature requirement for reaction, CO_2 conversion, CH_4 selectivity, and CH_4 yield. For 3%Ru/GNK the maximum CO_2 conversion that we are getting is 51.6% and 97.7% selectivity of CH_4 and 41.8% CH_4 of yield. Our CO_2 TPD data emphasized the significance of catalyst basicity in CO_2 methanation, with the order of CO_2 adsorption capacity being 3% Ru/GNK > 5% Ru/GNK > 1% Ru/GNK. Furthermore, our study

View Article Online
DOI: 10.1039/D5CY00021A

explored the importance of maintaining optimal reactant gas flow rates to maximize CO_2 conversion and CH_4 selectivity at lower temperatures. Our optimized conditions for CO_2 methanation were established as GHSV=20,000 h^{-1}, CO_2 : H_2 = 1 : 4, and a temperature of 350°C. Notably, long-term stability testing of the catalyst revealed only a 3% decrease in CO_2 conversion and a 2% decrease in CH_4 selectivity after 20 hours of testing under the optimized conditions. This decrease was attributed to the deposition of a small amount (0.078mg/g_{cat}) of coke (C) during the reaction. In conclusion, this research provides valuable insights into using geopolymer-based catalysts for CO_2 methanation, with the 3% Ru/GNK catalyst emerging as a promising candidate for sustainable methane production.

DATA AVAILABILITY

The data supporting this article have been included as part of the Supplementary Information.

ACKNOWLEDGMENT

MK and SS acknowledges Indian Institute of Technology Gandhinagar for providing Central Instrumentation Facility for carrying out the characterization. MK is thankful to IIT Gandhinagar for fellowship. SS acknowledges Department of Science and technology and Science and Engineering Research Board sponsored research project - CRG/2022/004926 and CEFIPRA sponsored project - 64T2B for funding.

REFERENCES

1 P. Frontera, A. Macario, M. Ferraro and P. Antonucci, *Catalysts*, 2017, **7**, 59.
2 A. Arsalis, P. Papanastasiou and G. E. Georghiou, *Renewable Energy*, 2022, **191**, 943–960.
3 Z. Li, P. Guo, R. Han and H. Sun, *Energy Exploration & Exploitation*, 2019, **37**, 5–25.
4 C. Mebrahtu, F. Krebs, S. Abate, S. Perathoner, G. Centi and R. Palkovits, in *Studies in Surface Science and Catalysis*, Elsevier, 2019, vol. 178, pp. 85–103.

5 C. Q. Pham, M. B. Bahari, P. S. Kumar, S. F. Ahmed, L. Xiao, S. Kumar, A. S. Qazaq, F. J. Siang, H.-T. Tran, A. Islam, A. Al-Gheethi, Y. Vasseghian and D.-V. N. Vo, *Environ Chem Lett*, DOI:10.1007/s10311-022-01483-0.
6 L. Falbo, M. Martinelli, C. G. Visconti, L. Lietti, C. Bassano and P. Deiana, *Applied Catalysis B: Environmental*, 2018, **225**, 354–363.
7 L. Shen, J. Xu, M. Zhu and Y.-F. Han, *ACS Catal.*, 2020, **10**, 14581–14591.
8 C. Liang, L. Zhang, Y. Zheng, S. Zhang, Q. Liu, G. Gao, D. Dong, Y. Wang, L. Xu and X. Hu, *Fuel*, 2020, **262**, 116521.
9 K. Ghaib, K. Nitz and F.-Z. Ben-Fares, *ChemBioEng Reviews*, 2016, **3**, 266–275.
10 K. Aimdate, A. Srifa, W. Koo-amornpattana, C. Sakdaronnarong, W. Klysubun, S. Kiatphuengporn, S. Assabumrungrat, S. Wongsakulphasatch, W. Kaveevivitchai, M. Sudoh, R. Watanabe, C. Fukuhara and S. Ratchahat, *ACS Omega*, 2021, **6**, 13779–13794.
11 A. Singhal, B. P. Gangwar and J. M. Gayathry, *Applied Clay Science*, 2017, **150**, 106–114.
12 Geopolymers in: Journal of Thermal Analysis and Calorimetry Volume 37 Issue 8 (2005), https://akjournals.com/view/journals/10973/37/8/article-p1633.xml, (accessed November 17, 2022).
13 J. Davidovits and M. Davidovics, *How Concept Becomes Reality.*, 1991, **36**, 1939–1949.
14 E. Kłosek-Wawrzyn, J. Małolepszy and P. Murzyn, *Procedia Engineering*, 2013, **57**, 572–582.
15 M. Thommes, K. Kaneko, A. V. Neimark, J. P. Olivier, F. Rodriguez-Reinoso, J. Rouquerol and K. S. Sing, *Pure and applied chemistry*, 2015, **87**, 1051–1069.
16 V. B. Saptal, T. Sasaki and B. M. Bhanage, *ChemCatChem*, 2018, **10**, 2593–2600.
17 M. K. Awasthi, R. K. Rai, S. Behrens and S. K. Singh, *Catal. Sci. Technol.*, 2021, **11**, 136–142.
18 A. G. Shastri and J. Schwank, *Journal of Catalysis*, 1985, **95**, 271–283.
19 H. Ooka, J. Huang and K. S. Exner, *Frontiers in Energy Research*.
20 M. Tommasi, S. N. Degerli, G. Ramis and I. Rossetti, *Chemical Engineering Research and Design*, 2024, **201**, 457–482.
21 A. Bisht, A. Sihag, A. Satyaprasad, S. S. Mallajosyala and S. Sharma, *Catal Lett*, 2018, **148**, 1965–1977.
22 K. Stangeland, D. Kalai, H. Li and Z. Yu, *Energy Procedia*, 2017, **105**, 2022–2027.
23 H. Wan, Y. He, Q. Su, L. Liu and X. Cui, *Fuel*, 2022, **319**, 123627.
24 N. Czuma, K. Zarębska, M. Motak, M. E. Gálvez and P. Da Costa, *Fuel*, 2020, **267**, 117139.

Data Availability Statement

View Article Online
DOI: 10.1039/D5CY00021A

The data supporting this article have been included as part of the Supplementary Information.